PNAS RESEARCH ARTICLE | IMMUNOLOGY AND INFLAMMATION

LPA suppresses T cell function by altering the cytoskeleton and disrupting immune synapse formation

Kimberly N. Kremer[a], Alan Buser[a], Dean Thumkeo[b], Shuh Narumiya[b], Jordan Jacobelli[a,c], Roberta Pelanda[a,d], and Raul M. Torres[a,d,1]

Edited by Michael Dustin, University of Oxford, Oxford, United Kingdom; received October 19, 2021; accepted February 16, 2022

Cancer and chronic infections often increase levels of the bioactive lipid, lysophosphatidic acid (LPA), that we have demonstrated acts as an inhibitory ligand upon binding LPAR5 on CD8 T cells, suppressing cytotoxic activity and tumor control. This study, using human and mouse primary T lymphocytes, reveals how LPA disrupts antigen-specific CD8 T cell:target cell immune synapse (IS) formation and T cell function via competing for cytoskeletal regulation. Specifically, we find upon antigen-specific T cell:-target cell formation, IP3R1 localizes to the IS by a process dependent on mDia1 and actin and microtubule polymerization. LPA not only inhibited IP3R1 from reaching the IS but also altered T cell receptor (TCR)–induced localization of RhoA and mDia1 impairing F-actin accumulation and altering the tubulin code. Consequently, LPA impeded calcium store release and IS-directed cytokine secretion. Thus, targeting LPA signaling in chronic inflammatory conditions may rescue T cell function and promote antiviral and antitumor immunity.

LPA | TCR | cytoskeleton | immune synapse | IP3R1

Significance

Cancers and chronic infectious pathogens often evade immune-mediated elimination by suppressing T cell function via engaging inhibitory receptors expressed on T cells. The phospholipid lysophosphatidic acid (LPA) is often increased systemically from basal concentrations upon development of cancer and chronic infections. We previously showed that, at these elevated concentrations, LPA suppresses the ability of CD8 T cells to kill malignant cells and to control tumor growth. Here, we demonstrate that LPA signaling suppresses T cell function via disrupting T cell receptor–induced cytoskeletal dynamics, immune synapse formation, signal transduction, and the tubulin code. This report identifies a targetable mechanism of receptor-mediated inhibition of T cell function that could be used in combination therapies to enhance antitumor and antiviral immunity.

Cancers and pathogens that establish chronic infections evade CD8 T cell immunity by suppressing T cell effector functions and often via the engagement of diverse inhibitory receptors expressed on T cells. These inhibitory receptors utilize various strategies to impede T cell effector functions, including competition for ligands, recruitment of phosphatases, and induction of apoptosis (1–3). Here, we describe how lysophosphatidic acid (LPA), a bioactive phospholipid found at heightened levels in both chronic infections and cancer (4–8), inhibits early cytotoxic CD8 T cell antigen receptor (TCR) signaling by modifying the cytoskeleton to disrupt the localization of key signaling molecules to the immune synapse (IS).

T cell activation begins with TCR ligation to a cognate peptide–major histocompatibility complex (MHC) on an antigen presenting cell or target cell, which activates a tyrosine kinase cascade and early signaling events that are critical for T cell effector functions, including cytokine production and cytotoxicity. TCR signaling is initiated by Lck-mediated phosphorylation of CD3 molecules at immunoreceptor tyrosine-based activation motifs (ITAMs), which recruits the tyrosine kinase ZAP70 and begins a complex signaling cascade leading to activation of PLCγ1 that subsequently hydrolyzes phosphatidylinositol 4,5 bisphosphate into diacylglycerol (DAG) and inositol 1,4,5-trisphosphate (IP3) (9, 10). IP3 subsequently binds to the IP3R1 calcium channel on the endoplasmic reticulum (ER), which localizes near the TCR to permit directed calcium release (11, 12) to promote further signaling pathways necessary for cell activation, cytokine production, and CD8 T cell killing ability (13, 14). These early signaling events (within minutes of T cell activation) are accompanied by the complex rearrangement of the actin and microtubule cytoskeleton, which mediates the formation of the IS, the interface between the T cell and antigen presenting cell/target cell (15, 16). The development of a stable IS has been shown to rely on actin polymerization at the IS and stabilization of microtubules (MTs), two events mediated by the RhoA GTPase activating its effector, the formin, mDia1 (17–20). mDia1 contains formin homology domain 2 (FH2) domains, which not only nucleate actin to promote polymerization but also associate with MTs to regulate their stabilization (21, 22). These cytoskeletal changes promote the transport to the IS of key signaling molecules, as well as cargo (i.e., secretory granules containing cytokines and perforin), via motor proteins traversing along polymerized actin and/or stabilized MTs (17, 21–24). Coordinated orchestration of these early signaling events has been shown to be critical to the generation of an effective T cell response (17–19, 21–23).

LPA is a systemic extracellular phospholipid that has been implicated in various T cell–regulated diseases, including cancer, chronic infection, colitis, asthma, allergic airway inflammation, rheumatoid arthritis, and multiple sclerosis (4–7, 25–29). LPA is generated extracellularly by the phospholipase D enzyme, autotaxin (ATX), which is

Author contributions: K.N.K. and R.M.T. designed research; K.N.K. and A.B. performed research; K.N.K., D.T., S.N., and J.J. contributed new reagents/analytic tools; K.N.K., A.B., and R.M.T. analyzed data; K.N.K., R.P., and R.M.T. wrote the paper; K.N.K. and R.M.T. provided conceptualization and methodology; D.T., S.N., J.J., and R.P. reviewed and edited the manuscript; and R.P. contributed to conceptualization.

Competing interest statement: S.N. is a scientific advisor to Astellas Pharma, Inc. and Toray Co., Ltd.

This article is a PNAS Direct Submission.

[1]To whom correspondence may be addressed. Email: raul.torres@cuanschutz.edu.

This article contains supporting information online at http://www.pnas.org/lookup/suppl/doi:10.1073/pnas.2118816119/-/DCSupplemental.

Published April 8, 2022.

expressed and secreted by certain cell types and subsequently binds to integrins on the cell surface and converts abundantly available lysophosphatidylcholine into LPA. LPA can signal via six different G protein coupled receptors (GPCRs), referred to as LPA receptors (LPAR1 through 6), which are variably expressed on a variety of cell types and induce a number of processes, including migration, cell survival, proliferation, and inflammation (4–6). In fibroblasts and malignant cells, LPA has been well characterized to disrupt cellular adhesion and promote migratory capacity via the activation of RhoA and mDia, which subsequently polymerize actin and stabilize microtubules (30–32). LPA has also been shown to regulate various T cell functions, including chemokinesis, cytokine production, transendothelial migration, and T cell activation and differentiation via LPAR2, LPAR5, and/or LPAR6 (27, 29, 33–38).

A complex interplay has long been appreciated between the signaling pathways that emanate from TCR and GPCRs on T cells and was suggested by the ability of TCR signaling to arrest migrating T cells and for certain chemokine (G protein coupled) receptor signaling to supersede TCR signaling (39). More recently, signaling pathways initiated by the TCR have been shown to require association with a GPCR, independent of the GPCR ligand, to gain access to GPCR signaling effector molecules and fully activate signaling; conversely, GPCR signaling has also been shown to require the TCR to gain access to TCR-initiated kinase cascades (40–44). Furthermore, we previously demonstrated that LPA, signaling by LPAR5 on T cells, suppresses CD8 T cell killing of malignant cells both in vitro and in vivo by impeding localization of perforin to the IS (35, 38). Notably, systemic levels of LPA are found at significantly elevated levels in certain cancers and chronic viral infections and, at these heightened concentrations, likely act to suppress CD8 T cell immunity (4–8).

In this report, we demonstrate that LPA disrupts TCR-induced formation of the IS by disrupting TCR-induced actin and microtubule cytoskeletal changes and inhibiting the localization of key signaling molecules to the intended point of function. We further demonstrate that the cytoskeletal changes induced by LPA impair calcium store release and directed cytokine secretion. Accordingly, by characterizing how a bioactive lipid, abundant in chronic infections and cancer, impairs T cell function, our data implicate manipulation of the ATX/LPA axis as a mechanism that could feasibly be used in combination therapies to promote T cell immunity.

Results

LPA Impairs TCR-Induced Release of Intracellular Calcium Stores by Interfering with IP3R1 Activity. TCR signaling results in a rapid increase in cytosolic calcium levels and is a consequence of both calcium release from intracellular ER stores and subsequent entry of extracellular calcium following activation of store-operated calcium channels (SOCs) in the plasma membrane (9, 10). We showed that LPA suppresses TCR-induced elevation of intracellular calcium levels in both murine (Fig. 1*A*) and human T cells (35, 38). LPA similarly inhibits B cell receptor (BCR)–mediated increased intracellular calcium levels in B cells via disrupting ER calcium store release (45). To determine whether LPA also suppresses TCR-induced

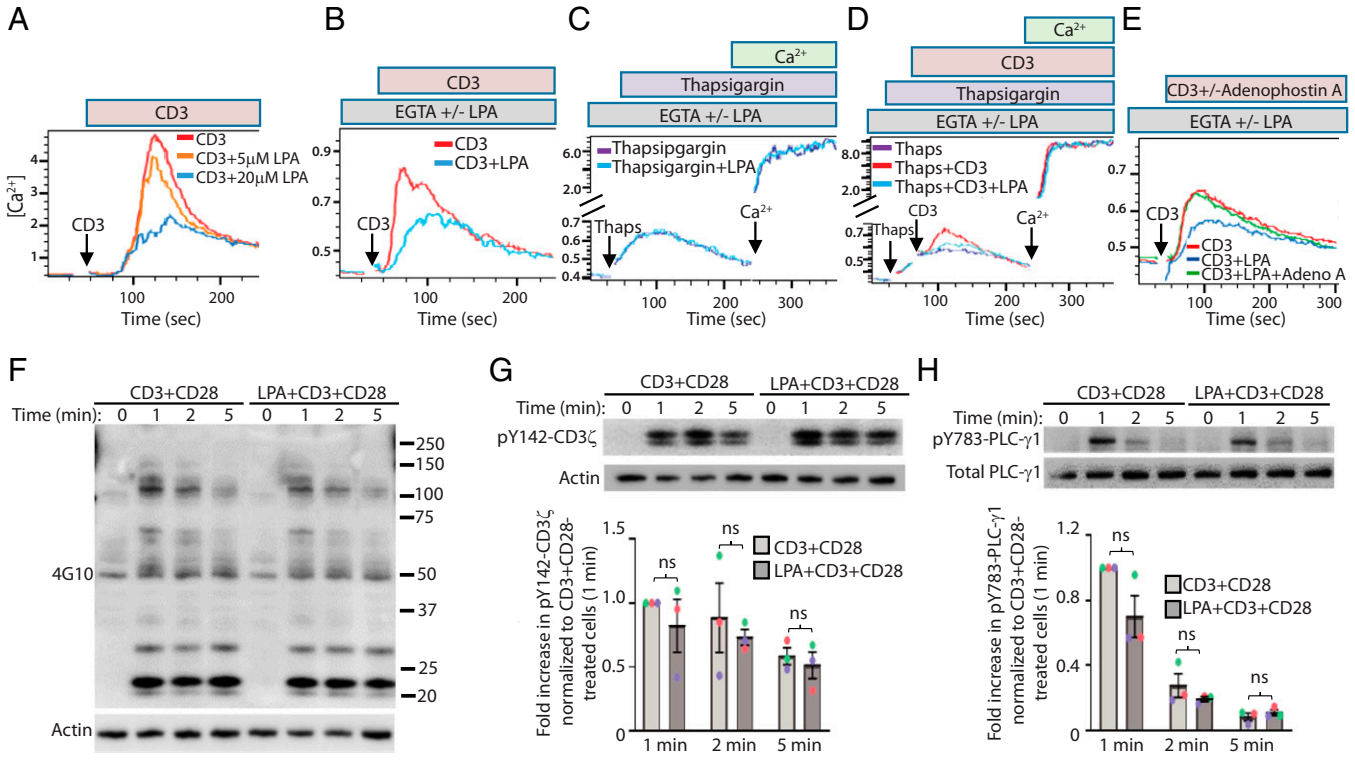

Fig. 1. LPA impairs TCR-induced release of intracellular calcium stores by interfering with IP3R1 activity. (*A–E*) Primary mouse CD8 T cells were loaded with Indo-1-AM and resuspended in (*A*) media or (*B–E*) 4 mM EGTA. At 0 min, cells were treated or not with 20 μM LPA, and anti–CD3-biotin with avidin and/or thapsigargin and/or adenophostin A and/or Ca^{2+} were added at the indicated times. Intracellular calcium concentrations were measured over time. Representative plots are shown for three independent experiments. (*F–H*) Primary human PBMC T cells were treated with biotinylated anti-CD3 with avidin cross-linking and anti-CD28 in the absence or presence of 20 μM LPA and immunoblotted for (*F*) global tyrosine phosphorylation (anti-phosphotyrosine, 4G10), (*G*) pY142-CD3ζ, or (*H*) pY783-PLC-γ1. Bar graphs represent three independent experiments with three different donor samples; dots (color-coded donors) and bars (mean) denote actin-normalized fold increase in phosphorylation also normalized to the anti-CD3 + anti-CD28–treated cells at the 1-min time point ± SEM. ns, no significant difference in the absence or presence of LPA as determined by Student's paired *t* test.

calcium release from intracellular stores, we induced TCR signaling via cross-linking by anti-CD3 monoclonal antibodies in the presence of 5 μM and 20 μM LPA. These concentrations represent physiological and pathological concentrations, respectively, found systemically and/or locally within the tumor microenvironment (46–51). Specifically, CD8 T cells were suspended in ethylene glycol tetraacetic acid (EGTA)-containing media to prevent extracellular calcium influx and allow intracellular calcium store release to be measured upon TCR activation in the absence or presence of LPA. LPA treatment of T cells clearly decreased TCR-induced calcium release from intracellular stores (Fig. 1*B*). Calcium in ER stores is depleted via the IP3R calcium channel upon engagement by IP3 produced by TCR-mediated activation of PLCγ1. Once depleted, ER calcium is replenished by an ER-resident Ca^{2+} ATPase that transports cytosolic Ca^{2+} back into the ER, which can be inhibited by thapsigargin. Accordingly, inhibition of TCR-mediated Ca^{2+} store release by LPA could feasibly manifest either by inhibiting IP3R-induced Ca^{2+} release or by enhancing Ca^{2+} ATPase activity. To discriminate between these two possibilities, we treated cells with thapsigargin in the presence of EGTA, which initiated a slow release of calcium stores resulting in elevated levels of cytosolic calcium and activation of SOCs in the plasma membrane, which mediated the influx of extracellular calcium upon the addition of sufficient extracellular calcium levels (at 4 min, after calcium store release) that evade EGTA-mediated chelation (Fig. 1*C*). LPA failed to both alter Ca^{2+} ATPase activity and inhibit extracellular calcium influx under these same conditions (Fig. 1*C*), suggesting that LPA does not directly enhance activity of the ER-resident Ca^{2+} ATPase or directly impair extracellular calcium influx. Interestingly, TCR stimulation of CD8 T cells in the presence of EGTA and thapsigargin increased further calcium store release, presumably via the binding of TCR-induced IP3 to the IP3R1 calcium channel on the ER. Importantly, LPA impaired TCR-induced calcium store release under these same conditions; however, LPA did not alter SOC-mediated extracellular calcium influx (Fig. 1*D*). Moreover, the addition of the IP3R1 agonist, adenophostin A, rescued the TCR-induced calcium store release and thus IP3R1 activity that was impaired in the presence of LPA (Fig. 1*E*). Together, these results show that LPA inhibits the TCR-induced release of calcium from intracellular stores by altering IP3R1 function and not altering the activity of the Ca^{2+} ATPase or SOCs.

To evaluate whether LPA also inhibited TCR-proximal signaling events that lead to suppressed calcium store release, we assessed the upstream TCR-induced kinase cascade, including activation of PLC-γ1, which generates the IP3 necessary to induce calcium mobilization via IP3R1 (9, 10). Using a general anti-phosphotyrosine antibody, we show that LPA does not alter global tyrosine phosphorylation in primary human T cells activated via anti-CD3 and anti-CD28 monoclonal antibodies (Fig. 1*F*). Tyrosine phosphorylation of the CD3ζ ITAMs is an early signaling event upon TCR binding to its cognate ligand (9, 10, 15, 16). Fig. 1*G* shows that the early tyrosine phosphorylation of Y142-CD3ζ, within ITAM 3, upon T cell activation, is also not significantly altered in the presence of LPA. Further downstream in the TCR kinase cascade, but immediately upstream of calcium mobilization, PLC-γ1 has been shown to be activated via tyrosine phosphorylation of Y783. Fig. 1*H* shows that LPA similarly does not impair the rapidly induced phosphorylation of Y783–PLC-γ1 upon T cell activation. Together these results indicate that LPA suppresses TCR-induced IP3R1 activity and thus calcium store release but does not alter the TCR-proximal signaling kinase cascade necessary to mobilize calcium.

IP3R1 Localizes to the IS of Antigen-Specific Conjugates; LPA Impairs IP3R1 IS Localization and Inhibits Actin Polymerization. Previously, IP3R1 has been shown to colocalize with the TCR in the Jurkat T cell line after induction of TCR signaling using anti-CD3 antibodies (11, 12). We asked whether IP3R1 similarly localized to the IS after initiation of antigen-specific TCR signaling between a primary effector cytotoxic CD8 T cell and its target cell. To accomplish this, we used mouse OT-I CD8 T cells, which express TCR transgenes specific for the SIINFEKL chicken ovalbumin (OVA) peptide (52). Effector cytotoxic T cells were generated by culturing transgenic T cells with SIINFEKL (N4)-pulsed splenocytes for 3 d followed by resting the stimulated OT-I T cells for 3 d in the presence of IL-2. Indeed, within 2 min of conjugation of antigen-specific OT-I effector CD8 T cells with antigen-specific target cells (N4-pulsed naïve B cells), we found that IP3R1 localized to the IS, indicated by phalloidin staining of polymerized actin (F-actin) at the IS (Fig. 2 *A*–*C*). Importantly, the presence of LPA significantly decreased the ability of IP3R1 to localize at the IS as determined by the ratio of synaptic IP3R1 compared to cytoplasmic IP3R1 relative to control (Fig. 2 *A*–*C*). Furthermore, the ratio of synaptic to cytoplasmic staining of F-actin was also decreased in LPA-treated cells compared to vehicle-treated cells (Fig. 2 *A*–*C*), suggesting that LPA also decreased TCR-induced actin polymerization at the IS. Utilizing phalloidin in a flow cytometric–based assay to measure total F-actin accumulation, independent of localization, we demonstrate that TCR signaling initiated via anti-CD3 and anti-CD28 treatment induced a rapid increase in F-actin in both naïve CD4 and CD8 primary human T cells (Fig. 2*D*). Importantly, LPA when present during TCR stimulation also impaired total polymerized actin in both naïve CD4 and CD8 T cells (Fig. 2 *D* and *E*). Together, these results show that IP3R1 localizes to the IS in antigen-specific conjugates. Furthermore, LPA interferes with both TCR-induced actin polymerization and localization of IP3R1 to the IS, which coincides with the ability of LPA to suppress intracellular calcium stores release by the TCR (Fig. 1).

Actin and Microtubule Polymerization Are Required for IP3R1 Localization to the IS. A common consequence of LPA receptor signaling by a variety of diverse cell types is the reorganization of the cytoskeleton (6, 25, 31, 53, 54); therefore, we considered the possibility that LPA may be altering the cytoskeleton of T cells in a manner that impairs IP3R1 localization to the IS upon T cell activation. The localization of IP3R1 has been attributed to rely on either actin- or microtubule-interacting proteins in different cell types (55, 56); however, the role of actin and microtubules in mediating IP3R1 localization in T cells has not yet been described. To assess whether actin polymerization was required for IP3R1 localization to the IS, we used the cell-permeable potent inhibitors of actin polymerization, cytochalasin D (cyto D) and latrunculin A, during conjugate formation. We found that cyto D and latrunculin A significantly inhibited IP3R1 localization to the IS with substantial amounts of IP3R1 found distal to the IS (*SI Appendix*, Fig. S1 *A*–*D*). Together with data from Fig. 2, these results suggest that LPA-mediated disruption of actin polymerization at the IS likely contributes to impaired localization of IP3R1 to the IS.

In endothelial cells, IP3R1 has been described to move along microtubules leading to IP3R1 clustering that drives localized and directed calcium release to enhance robust downstream signaling (55, 56). To determine whether microtubule polymerization is necessary for IP3R1 localization to the IS in T cells,

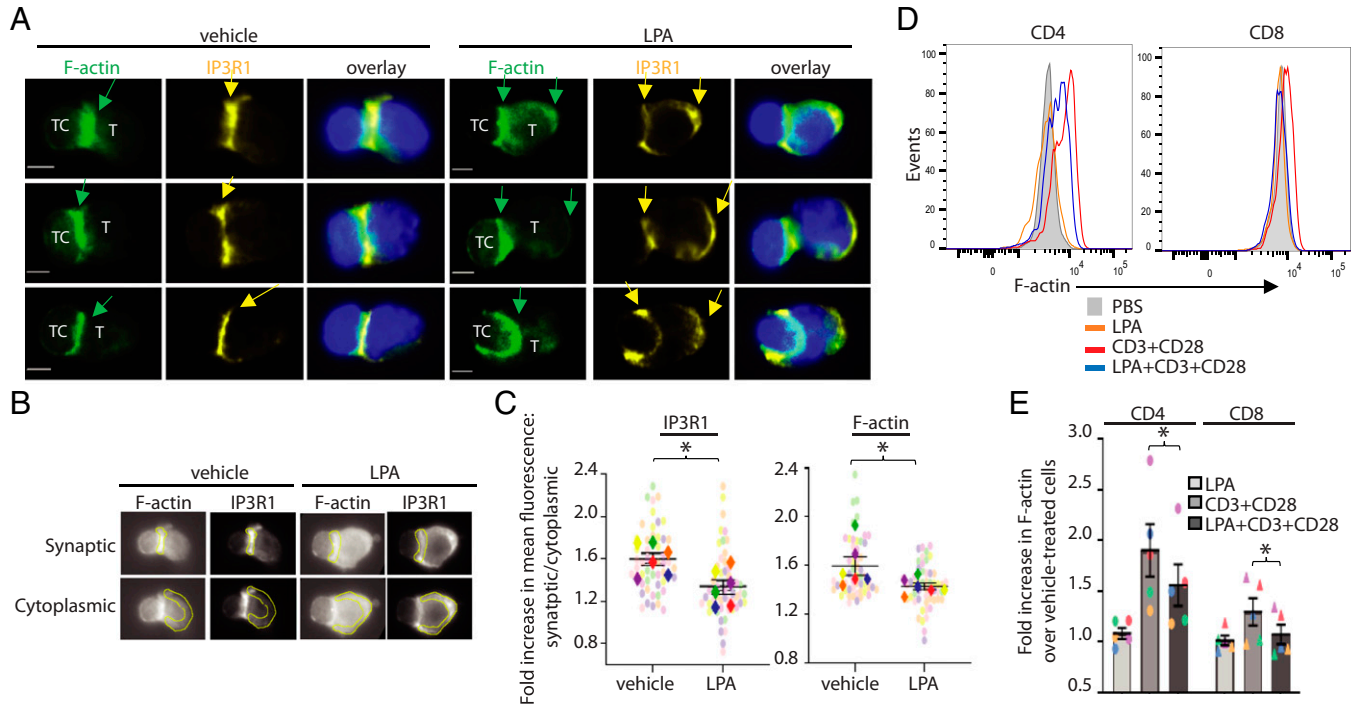

Fig. 2. IP3R1 localizes to the immune synapse of antigen-specific conjugates; LPA impairs IP3R1 IS localization and inhibits actin polymerization. (*A*) Antigen-specific effector OT-I CD8 T cells were conjugated with N4-peptide–pulsed B cells (target cells, TC) in the absence or presence of 20 μM LPA for 2 min. Conjugates were stained with phalloidin (green), anti-IP3R1 (yellow), and DAPI (blue) with "T" indicating antigen-specific effector OT-I T cells and "TC" indicating peptide-pulsed target B cells. Representative conjugates are shown. (Scale bars, 3 μm.) (*B*) Representative images with "synaptic" and "cytoplasmic" regions of interest (ROIs) are shown for F-actin and IP3R1 staining in the absence and presence of LPA. (*C*) SuperPlots (86) summarizing the mean fold increase in the amount of fluorescence in the synaptic ROI/cytoplasmic ROI per cell (light circles) as well per biological replicate (bold diamonds) from six independent experiments for a total of 52 conjugates per condition ± SEM. Dots and diamonds are color coded to match each biological replicate (diamonds) with its individual cells (circles). *$P < 0.05$, paired Student's *t* test on biological replicates. (*D*) Flow cytometric measurement of F-actin accumulation in primary human naïve CD4 and CD8 T cells following stimulation with LPA, anti-CD3, and anti-CD28, or both for 1 min. (*E*) Summary bar graph of results from *D* with each dot (color-coded donor) and each bar (mean) denoting fold increase in F-actin compared to vehicle-treated cells from five different donors assayed on separate days ± SEM. *$P \leq 0.05$, Student's paired *t* test.

colchicine or nocodazole, rapid inhibitors of microtubule polymerization, were added to effector OT-I CD8 T cells upon formation of conjugates with peptide-pulsed target cells. *SI Appendix*, Fig. S1 *E–H* shows that inhibition of microtubule polymerization also decreased the ratio of synaptic vs. nonsynaptic IP3R1 staining. Thus, together these results indicate that both actin and microtubule polymerization are required for appropriate IP3R1 localization to the IS.

LPA Does Not Interfere with Antigen-Specific Cell Conjugate Formation, Cytotoxic T Cell Global Microtubule Polymerization, or Microtubule Organizing Center Polarization upon Target Cell Recognition. We next sought to determine whether LPA interferes with conjugation of antigen-specific OT-I CD8 T cells with their target cells. To address this, we differentially fluorescently labeled effector OT-I CD8 T cells and peptide-pulsed target cells prior to conjugate formation, and then, using flow cytometric analyses, compared the percent of T cell:target cell conjugates formed and stabilized over time in vehicle- or LPA-treated cells. *SI Appendix*, Fig. S2 *A* and *B* demonstrates that LPA treatment neither altered the percent of T cell:target cell conjugates formed compared to vehicle-treated conjugates, nor did it influence conjugate stability for the duration of the assay. In contrast, our results further demonstrate that inhibition of microtubule polymerization by nocodazole treatment did not prevent initial conjugate formation but did impair the ability of the conjugates to be sustained over time (*SI Appendix*, Fig. S2*B*). These combined results reveal that LPA does not impair the formation or stability of CD8 T cell:target cell conjugates and further suggests that, in contrast to nocodazole, LPA also does not appear to impact MT polymerization. Indeed, when directly evaluated using antibodies against α-tubulin to allow visualization of total cellular polymerized MT, we find that MT staining was similar between vehicle-treated and LPA-treated cells, in contrast to nocodazole-treated cells that showed impaired MT polymerization (*SI Appendix*, Fig. S2 *C* and *D*).

Polymerization of MT has been shown to be critical for proper polarization of the microtubule organizing center (MTOC) toward the IS (18, 21) and to facilitate MT delivery of secretory granules and cytokines to the target cell (57). Previously, utilizing Jurkat T cells activated by Raji B cells coated with the superantigen staphylococcal enterotoxin, the MTOC was shown to localize within 2 μm of the cell–cell contact site (58). Therefore, we used pericentrin staining to demarcate the MTOC and assessed its localization 2 min after antigen-specific T cell:target cell IS formation in the absence or presence of LPA. *SI Appendix*, Fig. S2 *E* and *F* reveals that the average distance between the MTOC and the center of the synapse (demarcated by the center of F-actin staining) was within 2 μM in both vehicle- and LPA-treated cells. Thus, taken together these results demonstrate LPA does not impair the formation or duration of T cell:target cell conjugate formation, MT polymerization, or the polarization of the MTOC toward the IS.

LPA Impairs Microtubule Detyrosination, But Not Acetylation, upon T Cell:Target Cell Conjugate Formation. Posttranslational modifications of MTs such as acetylation and detyrosination

critically regulate MT function by generating a "tubulin code" that not only determines the stability and dynamics of the MT but also regulates which MT-interacting proteins are able to bind and traffic signaling molecules or cargo along the MT (22, 59). In T cells, acetylation and detyrosination of MTs have been described to regulate MT stabilization and possibly the transport of the TCR, ZAP70, and other cargo (21, 24, 60, 61). LPA has been reported to induce acetylation (62) and detyrosination of MTs in nonlymphocyte cell types (22, 63). Accordingly, we assessed whether LPA treatment altered the TCR-induced tubulin code in effector CD8 T cells upon antigen-specific conjugate formation with target cells. Fig. 3*A* shows that in effector CD8 T cell:target cell conjugates, acetylated MTs concentrated near the IS as previously shown (61) and extended toward the distal end of the cell and did not appear to be altered by LPA treatment. To more accurately assess MT acetylation in the absence or presence of LPA, we relied on a flow cytometric–based assay (*SI Appendix*, Fig. S3*A*) to quantitate the level of MT acetylation in the antigen-specific conjugates. Fig. 3 *B* and *C* shows that upon T cell:target cell conjugate formation, MT acetylation is observed as early as 1 min and increased until 5 min when it reached a plateau. Importantly, LPA treatment did not significantly alter the level of MT acetylation in effector CD8 T cells upon conjugate formation (Fig. 3 *B* and *C*). We next assayed detyrosination of MTs by immunofluorescent microscopy using an antibody specific for detyrosinated tubulin. Fig. 3*D* reveals that detyrosinated MTs predominantly accumulated close to the IS of cell conjugates but also extended distally from the IS and by immunofluorescence microscopy looked similar in conjugates formed in the absence or presence of LPA. Using a flow-based MT detyrosination assay (*SI Appendix*, Fig. S3*B*), we find that when effector CD8 T cells established a conjugate with an antigen-specific target cell, MT detyrosination occurred as early as 1 min and plateaued between 2 and 5 min (Fig. 3 *E* and *F*). However, when conjugates were established in the presence of LPA, levels of MT detyrosination were significantly impaired in conjugated T cells compared to vehicle-treated cells (Fig. 3 *E* and *F*). In summary, *SI Appendix*, Figs. S2 and S3 indicate that LPA does not impair MT polymerization, MT acetylation, or MTOC polarization but instead diminishes detyrosination of MT, thus altering the cytotoxic CD8 T cell tubulin code.

LPA Alters the Dynamics and Localization of TCR-Induced RhoA Activation. Next, we sought to identify upstream signaling pathways targeted by LPA that disrupt IS formation and lead to reduced actin polymerization at, and IP3R1 localization to, the IS and diminished detyrosination of MTs. In fibroblasts, LPA is able to activate RhoA and its formin effector, mDia, to initiate both actin polymerization and MT detyrosination (21, 22, 30, 53, 64). TCR signaling has also been characterized to activate both RhoA and mDia1 to regulate actin polymerization and MT detyrosination (17, 19–21). Thus, we next measured the amount of active RhoA found in primary human T cells after treatment with LPA, anti-CD3/anti-CD28, or both treatments (Fig. 4 *A* and *B*). These data demonstrate that treatment with LPA alone results in significantly increased levels of active, GTP-bound RhoA within 1 min, which is moderately decreased by 2 min. In contrast, T cell activation with anti-CD3 and anti-CD28 did not induce GTP-bound RhoA at 1 min but did reach modest levels at 2 min. Interestingly, simultaneous LPA and TCR stimulation resulted in a significant decrease of RhoA-GTP levels compared to LPA alone but also a significant increase in RhoA-GTP levels attained by TCR activation alone, resulting in an intermediate level of active RhoA 1 min after stimulation. By 2 min, the levels of active RhoA leveled off between the different treatments. These results were consistent with four different healthy donor T cells assayed on separate days (Fig. 4 *A* and *B*). Thus, the presence of LPA alters the early dynamics and amount of TCR-induced RhoA activation.

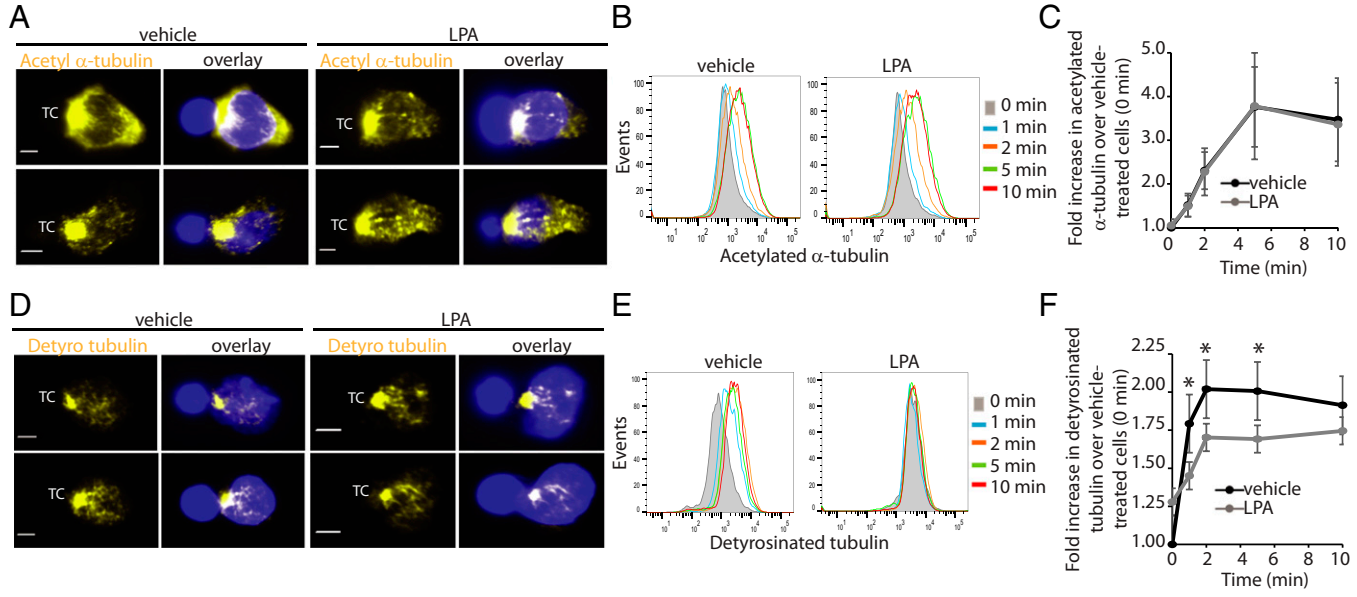

Fig. 3. LPA impairs microtubule detyrosination, but not acetylation, upon T cell:target cell conjugate formation. OT-I CD8 T cell:target cell conjugates were established in the absence or presence of 20 μM LPA and stained with DAPI (blue) and either (*A*) anti–acetyl-α-tubulin (after 2 min) or (*D*) anti-detyrosinated tubulin (after 10 min). Representative images are shown. (Scale bars, 3 μm.) Antigen-specific effector OT-I CD8 T cells were CFSE labeled and conjugated with eFluor670-labeled peptide-pulsed target cells in the absence or presence of 20 μM LPA, fixed, permeabilized, and stained for either (*B*) anti–acetyl-α-tubulin or (*E*) anti-detyrosinated tubulin prior to flow cytometric analysis at the indicated times after conjugate formation. Representative flow plots are shown. Line graphs summarize fold increase in (*C*) acetylation or (*F*) detyrosination of MTs in LPA treated (gray) over vehicle-treated (black) conjugates at 0 min ± SEM. $n = 4$, $^*P \leq 0.05$, Student's paired *t* test.

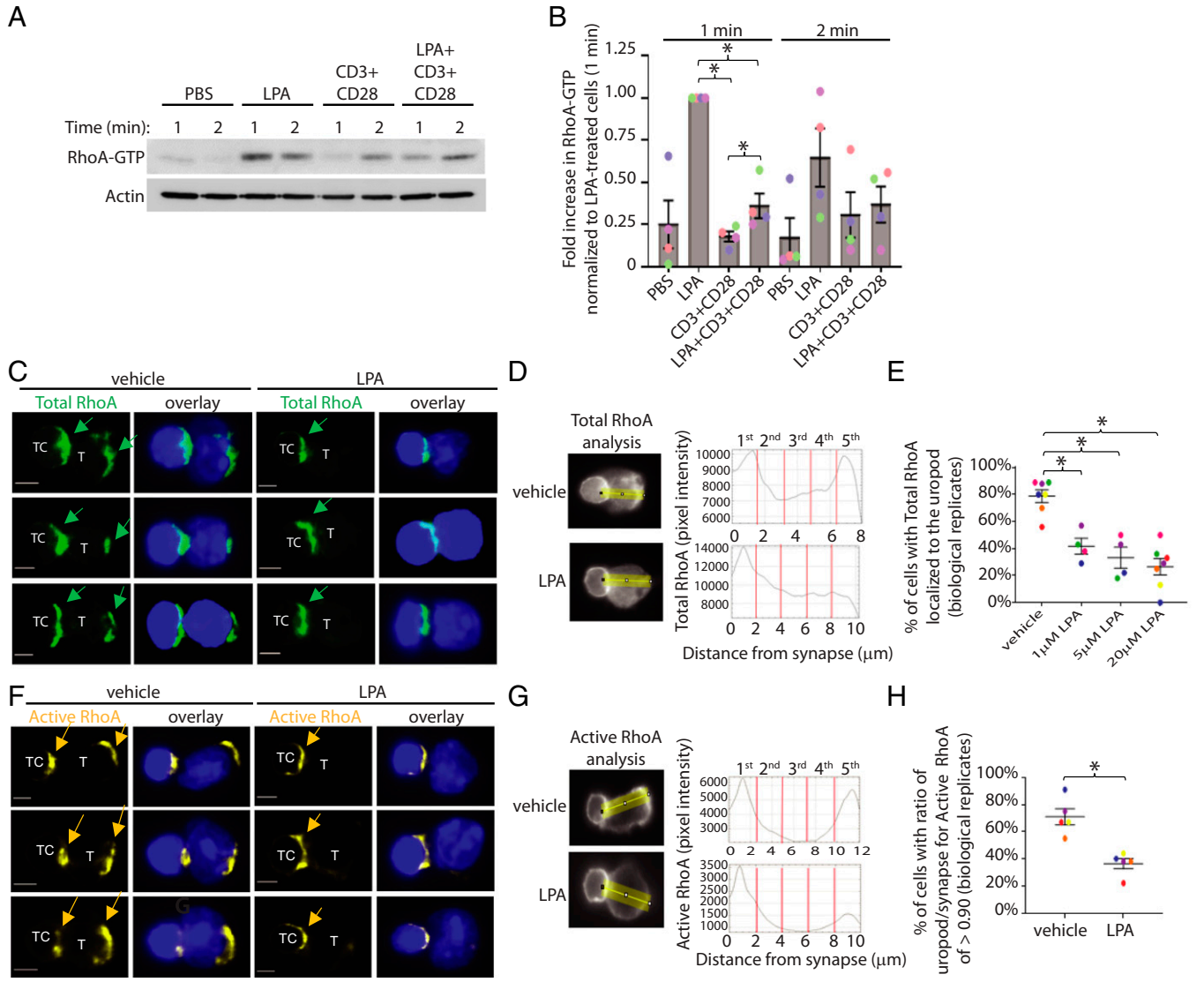

Fig. 4. LPA alters the dynamics and localization of TCR-induced RhoA activation. (*A*) Primary human PBMC T cells were treated for 1 to 2 min with 20 μM LPA, biotinylated anti-CD3 with avidin cross-linking, and anti-CD28 or both as indicated. Cell lysates were assayed for active RhoA-GTP and actin as control. Representative blots are shown. (*B*) Graph summarizes results in *A* with each dot (color-coded donor) and each bar (mean) denoting fold increase in RhoA-GTP normalized to LPA-treated cells at the 1-min time point for four different donors assayed on four different days, ± SEM, $P \leq 0.05$, Student's paired *t* test. (*C* and *F*) OT-I CD8 T cell:target cell conjugates were formed in the absence or presence of 20 μM LPA and stained with DAPI (blue) and either (*C*) total RhoA (green) or (*F*) active RhoA-GTP (yellow). (Scale bars, 3 μm.) (*D* and *G*) Representative images from *C* and *F* are shown with an ROI drawn from IS to the distal end of the cell, and representative pixel intensity plots (*y* axis) show either (*D*) total RhoA or (*G*) active RhoA-GTP staining and distance from the synapse (0 μm) over the indicated ROI. Red vertical lines divide the ROI over five regions for analysis. (*E*) Scatterplots summarize an LPA dose–response on altering RhoA localization in antigen-specific conjugates as in *D* with each dot denoting percent of cells per biological replicate with a higher level of fluorescence in region 5 than region 4, indicating percent of cells with total RhoA localized to the uropod from four to seven independent experiments for a total of 29 to 65 cells per condition, ± SEM, $P \leq 0.05$, Student's paired *t* test comparing biological replicates. (*H*) Scatterplot summarizes the results in *G* with each dot denoting the percent of cells per biological replicate with the ratio of active RhoA-GTP fluorescence at the uropod/synapse > 0.9, indicating percent of cells with a substantial amount of active RhoA-GTP localized to the uropod, for five independent experiments for a total of 39 to 48 cells per condition, ± SEM, *$P \leq 0.05$, Student's paired *t* test comparing biological replicates.

These results show that activation of RhoA in T cells can be rapidly induced by both LPA and TCR signaling and suggest that these receptors cross-regulate each other's ability to activate RhoA when both receptors signal simultaneously. Using immunofluorescence (IF) microscopy, we assessed whether LPA also influenced the localization of total and/or active RhoA induced upon TCR signaling in T cell:target cell conjugates. Fig. 4 *C–E* shows that in effector CD8 T cells, total RhoA not only localizes to the IS but is also found at the distal end of the cell, (defined here as the uropod) upon conjugate formation with antigen-specific target cells. In contrast, T cells treated with 1, 5, or 20 μM LPA harbored total RhoA primarily at the IS and lacked localization at the distal end of the cell (Fig. 4 *C–E*). Similarly, when active RhoA was visualized with an antibody specific for active GTP-bound RhoA, we again found active RhoA localized to the IS and uropod in antigen-specific T cell:-target cell conjugates, and again, LPA treatment restricted localization of active RhoA to only the IS (Fig. 4 *F–H*). Thus, these data indicate that LPA alters TCR-induced dynamics and localization of active RhoA, a key mediator of actin polymerization and MT detyrosination.

mDia1 Is Not Only Required for IS IP3R1 Localization But Also Fails to Efficiently Localize to the IS in the Presence of LPA. GTP-bound RhoA binds to the GTPase-binding domain on mDia1 releasing the N-terminal, inhibitory domain from the

C-terminal autoregulatory domain, which permits activation of mDia1 leading to actin polymerization and MT detyrosination via formin homology domains in a variety of cell types (30). Thus, we next asked whether mDia1 is necessary for IP3R1 localization to the IS upon conjugate formation. To address this, OT-I effector CD8 T cells were generated from *mDia1*-deficient OT-I mice; antigen-specific T cell:target cell conjugates were established; and IP3R1 localization to the IS was evaluated. Fig. 5 *A* and *B* demonstrates that in *mDia1*-deficient OT-I T cell:target cell conjugates, IP3R1 was clearly impaired in reaching the IS compared to wild-type (WT) OT-I T cells. Actin polymerization at the IS also decreased, but not significantly, in *mDia1*-deficient OT-I T cells compared to WT OT-I T cells (Fig. 5 *A* and *C*). In contrast, the formin FMNL1, also expressed in T cells and able to mediate actin polymerization (65), was not required for IP3R1 localization or actin polymerization at the IS upon conjugate formation (Fig. 5 *A*–*C*). Together, these results show that an mDia1 deficiency impairs IP3R1 localization and actin polymerization at the IS similar to LPA treatment (Fig. 2 *A* and *C*).

Given the similarities between mDia1 deficiency and LPA regulation of TCR-induced signaling outcomes as well as the ability of LPA to regulate TCR-induced RhoA activation, we next evaluated the localization of mDia1 in T cell conjugates. Upon antigen-specific T cell:target cell conjugate formation, mDia1 was found to localize along the entire IS (Fig. 5 D–F). In contrast, LPA treatment of conjugates resulted in the exclusion of mDia1 from the central region of the IS and instead mDia1 accumulated toward the periphery of the IS (Fig. 5 D–F). Thus, the presence of LPA during conjugate formation modifies the localization of mDia1 in activated T cells. Our combined results thus far suggest that LPA signaling alters TCR-induced RhoA activation, which disrupts mDia1 localization, resulting in impaired actin polymerization and MT detyrosination, both of which are critical for IP3R1 localization to the IS for effective calcium store release and T cell function.

LPA Impairs TCR-Induced IL-2 and IFNγ-Directed Cytokine Secretion But Not Multidirectional Secretion of TNFα. We have previously reported that LPA impairs antigen-specific CD8 T cell cytotoxic killing of target cells in vivo and in vitro via impeding the localization of perforin to the IS (38). The transport of perforin in CD8 T cells to the IS has been shown to proceed along MTs via motor proteins (66). Similarly, in

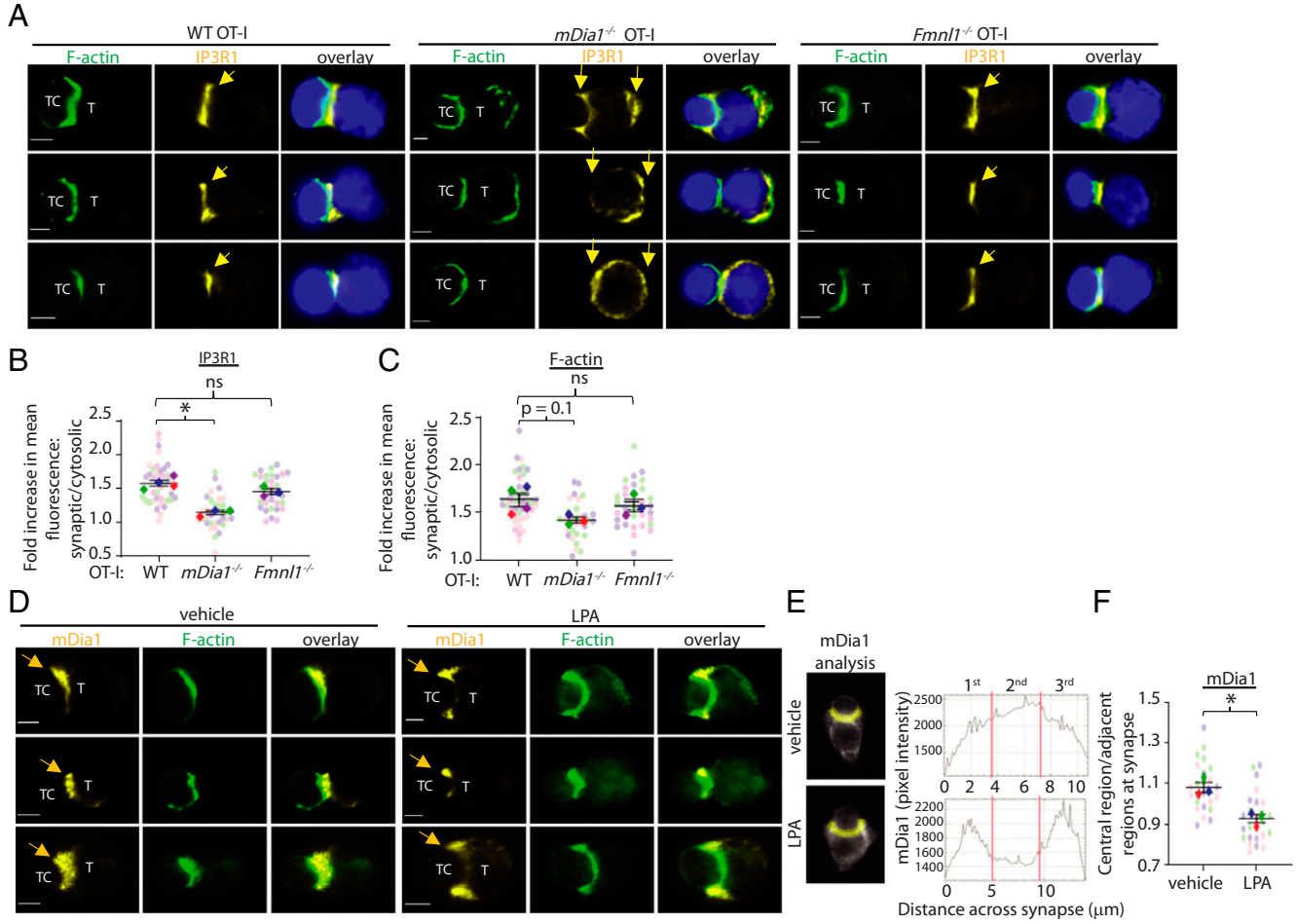

Fig. 5. mDia1 is not only required for IS IP3R1 localization but also fails to efficiently localize to the IS in the presence of LPA. (*A*) Antigen-specific OT-I effector CD8 T cells isolated from WT, *mDia1*$^{-/-}$, or *Fmnl1*$^{-/-}$ OT-I mice were conjugated with peptide-pulsed target cells for 2 min and stained with phalloidin (green), anti-IP3R (yellow), and DAPI (blue). Representative images are shown. (Scale bars, 3 μm.) SuperPlots summarize the mean fold increase in the amount of (*B*) IP3R1 or (*C*) F-actin fluorescence in the synaptic ROI/cytoplasmic ROI per cell (light circles) and per biological replicate (bold diamonds) as in Fig. 2 from three to four independent experiments for a total of 32 to 40 cells per condition, ± SEM, *$P < 0.05$, ns: not significant, Student's paired *t* test comparing biological replicates. (*D*) Representative images of antigen-specific OT-I effector CD8 T cells conjugated with peptide-pulsed target cells for 10 min in the absence or presence of 20 μM LPA and stained with phalloidin (green) and anti-mDia1 (yellow). (Scale bars, 3 μm.) (*E*) Representative images display ROI drawn along synapse (determined by F-actin staining) and representative pixel intensity plots (*y* axis) show mDia1 staining across the synapse over the indicated ROI. (*F*) SuperPlots summarize the ratio of mDia1 fluorescence in the central region compared to the average of the adjacent regions from three independent experiments for a total of 25 to 28 cells per condition, SEM, *$P < 0.05$, Student's paired *t* test comparing biological replicates.

CD4 T cells the IS-directed release of IL-2 and IFNγ has been reported to depend on actin regulators and an intact MT network, while multidirectional release of cytokines such as TNFα is neither dependent on actin nor MTs (66, 67). Thus, we assessed whether LPA was also able to regulate the release of the T cell effector cytokines IL-2, IFNγ, and TNFα. Primary human T cells were stimulated in vitro with anti-CD3 and anti-CD28 in the presence or absence of LPA and cytokines measured by enzyme-linked immunosorbent assay (ELISA) from culture supernatants 24 h later. Interestingly, we observed that, upon TCR stimulation of T cells isolated from seven different donors, LPA impaired the secretion of both IL-2 and IFNγ into the culture supernatant, but secretion of TNFα was not consistently altered by LPA (Fig. 6*A*). In contrast, intracellular flow cytometric staining of IL-2, IFNγ, or TNFα expressed by primary human naïve or memory, CD4, or CD8 T cells 20 to 24 h after activation revealed similar intracellular cytokine levels independent of LPA treatment (*SI Appendix*, Fig. S4 *A*–*C*). To account for the discrepancy between the ability of LPA treatment to inhibit cytokine secretion but not expression by TCR-stimulated primary human T cells, we evaluated intracellular cytokine localization in our antigen-specific murine T cell conjugates. Indeed, in OT-I CD8 effector T cell:target cell conjugates, IFNγ was found localized to the IS within 1 h, whereas TNFα was found in multiple vesicles throughout the cell, compatible with a multidirectional release (Fig. 6 *B*–*G*). In contrast, LPA treatment of T cell conjugates impaired the localization of IFNγ to the IS, but did not appear to alter the multidirected secretion pattern of TNFα.

LPA Alters the Optimal Level of TCR-Induced RhoA Activity Required for mDia1 and IFNγ Localization to the IS. We have shown that LPA increases early RhoA activity beyond TCR-induced RhoA activation (Fig. 4 *A* and *B*), thus we next sought to determine whether limiting the LPA-mediated increase in RhoA activity would rescue localization of mDia1 and IFNγ to the IS in antigen-specific conjugates in the presence of LPA. To limit RhoA activity, we treated effector CD8 T cells prior to target cell conjugate formation with a cell-permeable C3 transferase, which adenosine diphosphate (ADP) ribosylates and inactivates RhoA. We confirmed that total RhoA activity was decreased upon conjugate formation in C3 transferase-treated T cells via staining for active GTP-bound RhoA (Fig. 7*A*). Furthermore, inhibition of RhoA activity with C3 transferase

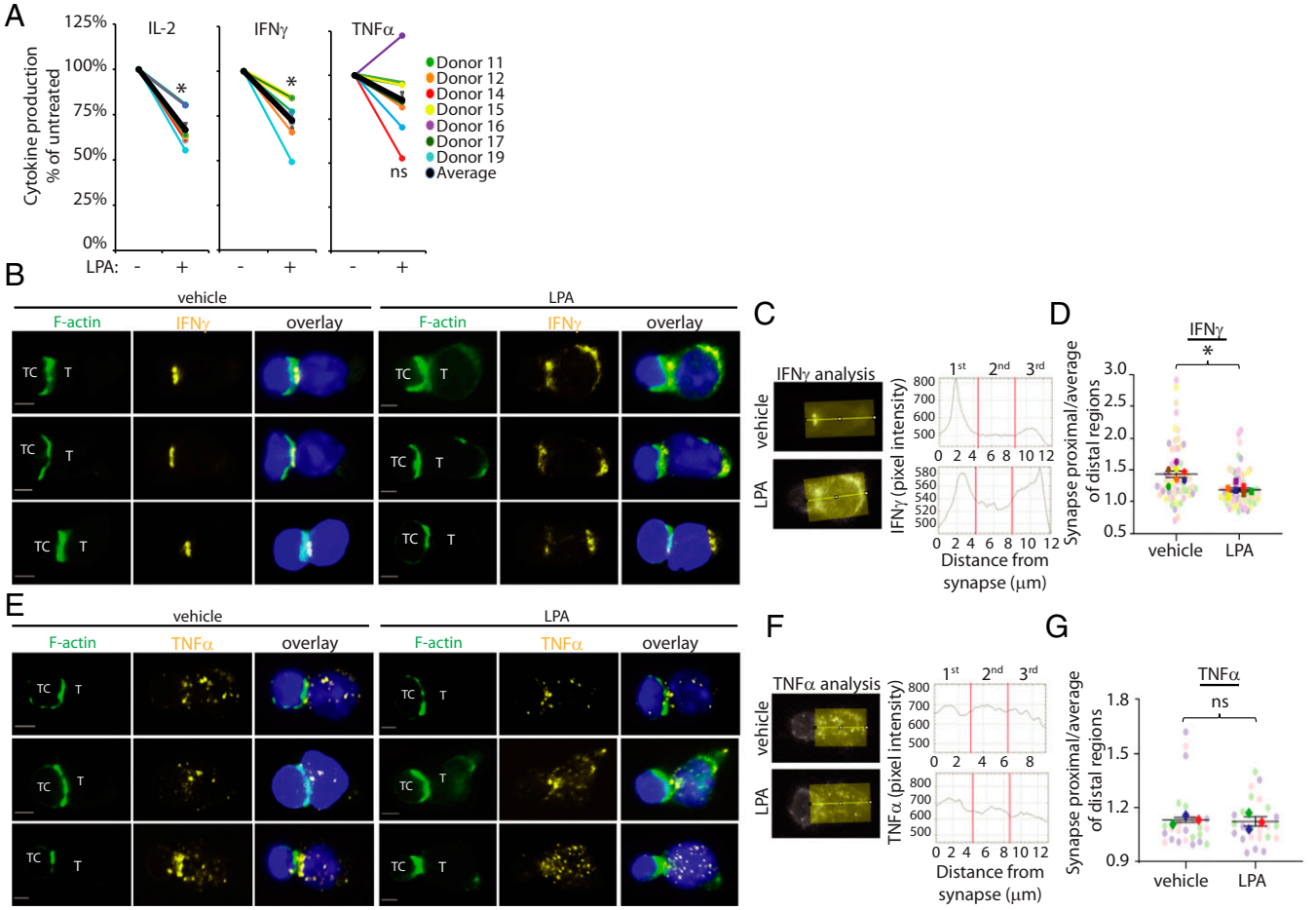

Fig. 6. LPA impairs TCR-induced IL-2 and IFNγ-directed cytokine secretion but not multidirectional secretion of TNFα. (*A*) Primary human PBMC T cells stimulated with plate-bound anti-CD3 and soluble anti-CD28 in the absence or presence of 20 μM LPA for 24 h and IL-2, IFNγ, and TNFα production measured in culture supernatants via ELISA. Graphs show relative percentage of cytokine measured in supernatant with anti-CD3 + anti-CD28 alone (−) or with (+) LPA. Results are shown for seven different donors and average (black line) ± SEM, $P \leq 0.05$, ns: not significant, Student's paired *t* test. (*B* and *E*) Representative images of antigen-specific OT-I effector CD8 T cell:target cell conjugates established for 1 h in the absence or presence of 20 μM LPA and stained with phalloidin (green), DAPI (blue), and either (*B*) anti-IFNγ or (*E*) anti-TNFα (yellow). (Scale bars, 3 μm.) (*C* and *F*) Representative images show ROI drawn to encompass the entire T cell, and representative pixel intensity plots (*y* axis) show (*C*) IFNγ or (*F*) TNFα fluorescence starting at the synapse (0 μM) and continuing across the cell. The red lines indicate the division of the cell into three equal regions for analysis. (*D* and *G*) SuperPlots show the ratio of the fluorescence of (*D*) IFNγ or (*G*) TNFα in the synapse proximal "region 1" compared to the average fluorescence of the two distal regions for seven and three independent experiments for a total of 62 to 64 and 22 to 26 cells per condition for *D* and *G*, respectively, ± SEM, $*P \leq 0.05$, Student's paired *t* test comparing biological replicates.

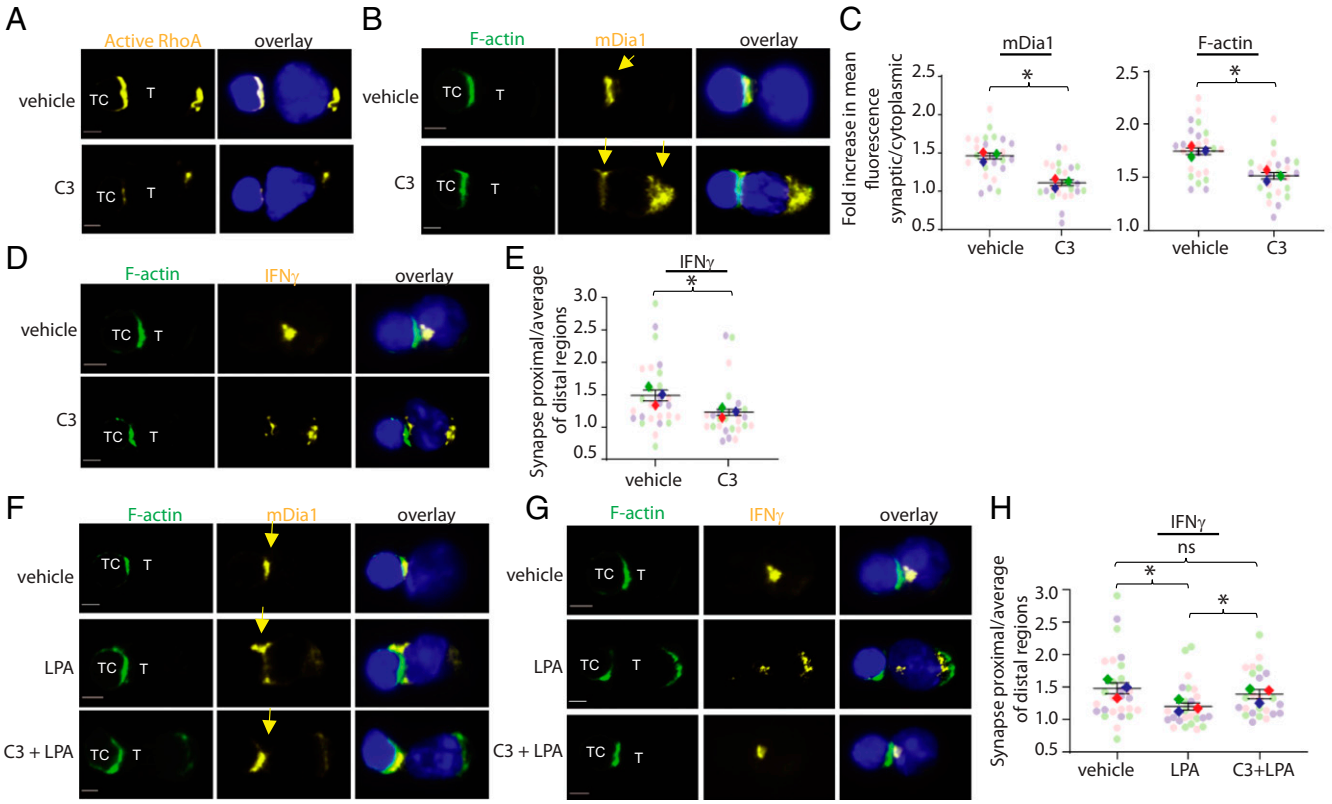

Fig. 7. LPA alters the optimal level of TCR-induced RhoA activity required for mDia1 and IFNγ localization to the IS. (*A–H*) Antigen-specific OT-I effector CD8 T cells were cultured for 2 h in the absence or presence of 4 μg/mL C3 transferase prior to conjugate formation with peptide-pulsed target cells with or without 20 μM LPA and stained with phalloidin (green), DAPI (blue), and either (*A*) active RhoA-GTP (yellow) or (*B* and *F*) mDia1 (yellow) or (*D* and *G*) IFNγ (yellow). Representative images are shown. (Scale bars, 3 μm.) (*C*) SuperPlots summarize the mean fold increase in the amount of mDia1 or F-actin fluorescence in the synaptic ROI/cytoplasmic ROI per cell (light circles) and per biological replicate (bold diamonds) as in Fig. 2 from three independent experiments for a total of 24 to 26 cells per condition, ± SEM, *$P \leq 0.05$, Student's paired *t* test comparing biological replicates. (*E* and *H*) SuperPlots show the ratio of the fluorescence of IFNγ in the synapse proximal "region 1" compared to the average fluorescence of the two distal regions as in Fig. 6 for three independent experiments for a total of 25 to 27 cells per condition, ± SEM, *$P \leq 0.05$, ns: not significant, Student's paired *t* test comparing biological replicates.

impaired localization of mDia1, F-actin accumulation, and IFNγ to the IS in T cell:target cell conjugates (Fig. 7 *B–E*). Finally, we show that limiting RhoA activity in T cell:target cell conjugates in the presence of LPA with C3 transferase, to levels presumably attained by TCR-induced signaling alone, promotes mDia1 and IFNγ localization to the IS (Fig. 7 *F–H*). Together, the results from this report are summarized in our proposed model (Fig. 8 and *SI Appendix*, Fig. S5) and indicate that LPA impairs TCR-induced IL-2 and IFNγ secretion likely via altering RhoA activation and disrupting mDia1 localization to the IS. Consequently, there is reduced actin polymerization and MT detyrosination, which are both required for IP3R1 localization to the IS and efficient IP3R1 activation, resulting in decreased calcium store release and impaired localization of perforin and directed cytokine release at the IS.

Discussion

Viruses and malignancies often co-opt the expression or secretion of key regulatory molecules in order to promote viral spread and tumor growth and evade elimination by the adaptive immune response. ATX expression and subsequent LPA production are elevated by various viruses and multiple malignancies (4–8). LPA not only stimulates the survival and proliferation of infected and malignant cells (6, 7), but LPA also regulates the cytoskeleton to promote cellular migration and chemokinesis in a variety of cell types (4–6, 27, 34, 36, 37, 54) via binding LPAR1, 2, and 4 through 6, all of which are capable of associating with $G\alpha_{12/13}$ to promote RhoA activation (68). Cytoskeletal regulation by LPA involves several of the same signaling molecules that the TCR utilizes to induce synapse formation when encountering an antigen presenting cell or target cell (17, 19, 27, 31, 53, 54, 69). Thus, in an LPA-rich environment, we envision that TCR signaling, induced by T cells encountering their cognate peptide–MHC, likely competes with LPAR signaling pathways to promote the unique cytoskeletal changes necessary to drive T cell effector functions. Indeed, we describe in this report, an inhibitory mechanism utilized by LPA to suppress cytokine secretion, and ultimately cytotoxicity (38), by subverting IS formation and the localization of key signaling molecules to the IS.

In this study, we sought to identify the TCR-induced signaling mechanisms disrupted by LPA signaling, and in so doing, we also characterize TCR-induced, cytoskeletal signaling mechanisms that promote localization of IP3R1 to the IS. As an intracellular store calcium channel, IP3R1 localization to the IS would permit efficient activation of IP3R1 and robust delivery of calcium to the site where TCR signaling is engaged to activate calcium-dependent channels and signaling molecules necessary for T cell activation (11, 12). Here, we document that upon antigen-specific T cell activation of primary effector CD8 T cells, IP3R1 localizes to the IS. We additionally show that this IP3R1 localization to the IS is not only dependent on mDia1 but also its actin and MT polymerization effector functions. Moreover, the activity of RhoA, an indirect mediator of both actin polymerization and MT detyrosination, was shown

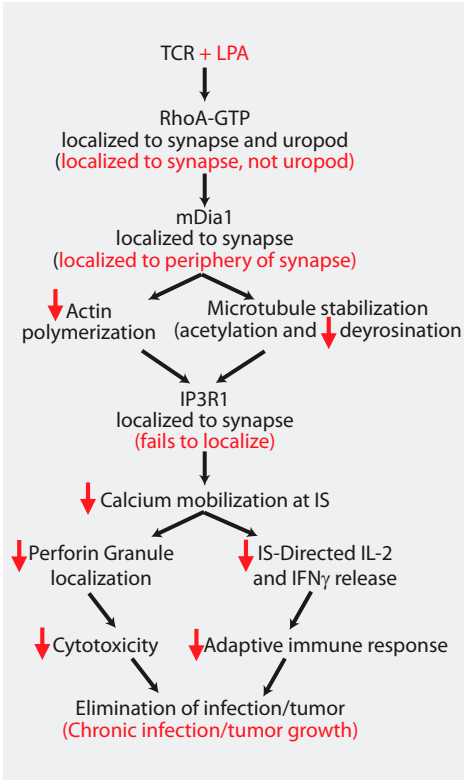

Fig. 8. Proposed mechanistic diagram of antigen-specific T cell activation in the presence and absence of LPA.

to be necessary for both mDia1 localization to the IS and for IS-directed secretion of IFNγ. We further reveal that total and active RhoA were localized at both the IS and uropod upon antigen-specific T cell activation. GTP-bound active RhoA has been found localized to the IS in CD4:target cell conjugates (70) and to both the IS and uropod in a migrating CD4 T cell line (71). While active RhoA in CD8:target cell conjugates at the IS is likely important in promoting actin polymerization, a role for active RhoA at the T cell distal end is not clear but may either prepare the T cell to retract from the current target cell as it searches for the next target (72) or reflect the uropod acting as an anchor to keep the T cell from migrating away from the target cell (73). Using both IF microscopy and flow cytometric analyses of effector CD8 T cell:target cell conjugates over time, we show that changes in acetylation and detyrosination of MTs, which alter the T cell tubulin code, occur within 1 to 2 min after conjugate formation. Thus, this shows that regulation of the cytoskeleton and tubulin code are necessary for IP3R1 localization to the IS as well as the subsequent calcium flux that occurs within seconds of T cell activation.

Here, we describe the ability of LPA signaling to impair T cell function by disrupting IS formation, modifying the tubulin code, and impeding the localization of key signaling molecules to the IS. LPA treatment of primary T cells not only altered the level and kinetics of RhoA activation but also altered the location of active RhoA upon T cell activation. Furthermore, upon LPA treatment, mDia1, a direct RhoA effector, failed to localize to the central region of the IS near the MTOC. Several scaffolding, mDia1-interacting molecules, including IQGAP1, CLIP170, and EB1/EB3, have been described to not only signal upon both TCR and LPA stimulation but also to regulate F-actin and/or MT dynamics in different cell types (74–77). Thus, TCR-induced mDia1 localization is likely dependent on a signaling complex involving RhoA-GTP and several F-actin and MT scaffolding proteins that is perturbed when LPA competes for regulation of these same molecules to reorganize the cytoskeleton. We show here that the inability of mDia1 to efficiently localize to the IS in the presence of LPA likely impairs the ability of mDia1 to induce robust F-actin accumulation and MT detyrosination ultimately impairing IP3R1 localization to the IS, which is required for efficient, directed calcium store release that drives the TCR signaling pathways necessary to promote transport of perforin and cytokines to the IS. This inhibitory LPA signaling may occur via LPAR2, LPAR5, and/or LPAR6 that are expressed on naïve and activated human and mouse T cells (38). We have established that inhibition of TCR-induced calcium mobilization and ERK phosphorylation are suppressed specifically by LPAR5 signaling (38). However, this study does not rule out the possibility that LPAR2 and/or LPAR6 may also contribute to impeding IS formation and cytokine secretion in antigen-specific CD8 T cell conjugates, which will require further investigation. Nonetheless, LPA signaling thwarts TCR signaling by altering the localization and activation of key signaling molecules necessary for the cytoskeletal rearrangements critical to promote T cell function.

LPA, unlike other inhibitors of T cell signaling (78–80), did not disrupt the TCR-induced proximal signaling cascade that mediates activation of PLC-γ1. Interestingly, LPA also did not impair all TCR-induced cytoskeletal changes, leaving T cell:target cell conjugation and MTOC polarization intact. T cell:target cell conjugate formation relies on activation of the integrin LFA-1 which is regulated by the proximal TCR kinase cascade (81, 82) (not influenced by LPA) and F-actin accumulation (81, 83) (which occurs to a lesser extent in LPA-treated cells). Interestingly, we show here that MT polymerization is not required for T cell:target cell conjugate formation but is necessary to maintain conjugate formation over time. Furthermore, MTOC polarization has been shown to be dependent on phosphorylation and activation of Src family kinases (84, 85) (TCR-proximal signaling events not affected by LPA), detyrosinated MT (18), and mDia1 (69) in Jurkat T cells. Our results suggest that detyrosinated MT may not be necessary for MTOC polarization in an antigen-specific manner; however, LPA did not completely inhibit detyrosination of MT, which was seen localized near the MTOC, perhaps suggesting that limited detyrosination at the MTOC is sufficient for MTOC polarization. The modified localization of mDia1 to the IS in response to LPA may also have been sufficient for MTOC polarization. Nonetheless, the disruption of activation kinetics and localization of key signaling molecules in the presence of LPA were significant enough to effectively limit F-actin accumulation at the IS, MT detyrosination, IP3R1 localization to the IS, and calcium store release that together appear to impair the transport of cytokine containing vesicles via disrupting interactions with actin-binding and MT motor proteins.

In summary, this report provides mechanistic insight into how LPA, a lipid abundant in cancer and chronic infections, impairs T cell functions in a manner that is clearly distinct from other inhibitory receptors. Accordingly, the LPA–LPAR axis represents an alternative signaling pathway that could be targeted, as a combination therapy, to enhance T cell cytokine production and killing ability in the LPA-rich environments induced by chronic viral infections and malignancies.

Materials and Methods

Mice. C57BL/6 (stock no. 000664, The Jackson Laboratory), OT-I mice (stock no. 003831), *mDia1*$^{-/-}$ OT-I mice [generated by crossing *mDia1*$^{-/-}$ mice (20) with OT-I mice], and *Fmnl1*$^{-/-}$ OT-I mice (65) were bred and housed at the University

of Colorado Anschutz Medical Campus Vivarium (Aurora, CO). All procedures with animals were approved by the University of Colorado Institutional Animal Care and Use Committee.

Intracellular Calcium Measurements. Erythrocyte-lysed spleens from C57BL/6 mice were resuspended at 20×10^6 cells per milliliter in RPMI with 2.5% fatty-acid free bovine serum albumin (BSA), and stained with 5 μM Indo-1-AM and anti–CD8-PE for 30 min at 37 °C. Cells were washed and resuspended at 5×10^6 cells per milliliter. For calcium measurements, LPA was added or not at 0 min and a baseline was gathered for 30 s at which time 10 μg/mL anti–CD3-biotin and 20 μg/mL avidin were added and intracellular calcium was measured. To assess calcium store release and extracellular calcium influx, cells were resuspended in 4 mM EGTA, and 1 μM thapsigargin, 10 μM adenophostin A, and/or 8 mM Ca^{2+} were added at the indicated times.

Human Peripheral Blood Mononuclear Cell T Cell Stimulation and Analysis. For biochemical assays, total T cells were stimulated with 1 μg/mL anti-CD3 cross-linked with avidin and 20 μg/mL soluble anti-CD28 for the indicated time, lysed, and immunoblotted for the indicated protein. To assay F-actin accumulation via flow cytometry, total T cells were stimulated, fixed in 4% paraformaldehyde, permeabilized with phosphate-buffered saline (PBS)/0.1% saponin/0.5% BSA for 10 min, stained with cell surface receptors (CD4, CD8, and CD45RA [naïve]) and phalloidin, and analyzed via flow cytometry. To assay active RhoA-GTP, total T cells were stimulated, lysed in Mg+ lysis/wash buffer (MLB) buffer (Millipore) with protease inhibitors, and centrifuged to remove nuclei. Supernatants were rotated with 10 μg of GST-Rhotekin Rho-binding domain (Millipore) for 30 min at 4 °C, washed, boiled in sample buffer, and immunoblotted for RhoA. To assay cytokine production, total T cells were stimulated with 1 μg/mL plate-bound anti-CD3 and 12.5 μg/mL soluble anti-CD28 in the presence or absence of LPA for 1) 24 h prior to supernatant harvest for analysis via ELISA or 2) 16 to 18 h prior to addition of 10 μg/mL brefeldin A for 4 h at 37 °C followed by cell surface receptor staining, intracellular fixation, and permeabilization (88-8824-00, eBiosciences) and then staining for the indicated cytokines.

Generation of Antigen-Specific OT-I Effector Cells and Target Cells. OT-I CD8 T cells from OT-I transgenic mice (WT, *mDia1*$^{-/-}$, or *Fmnl1*$^{-/-}$ on an OT-I background) were stimulated by pulsing erythrocyte-lysed splenocytes with 2 μg/mL of SIINFEKL (N4) peptide in complete media with penicillin/streptomycin for 3 d at 37 °C. After incubation, cells were cultured in fresh media with IL-2 at 100 U/mL for an additional 3 d. Peptide-activated $CD8^+$ T cells were isolated via Ficoll separation and used in assays with target cells. To generate antigen-specific target cells, B cells were negatively enriched using magnetic anti-CD43 beads from C57BL/6 splenocytes and loaded with 2 μg/mL of SIINFEKL peptide for 1 to 2 h at 37 °C and washed twice prior to use as target cells.

Formation of Effector T Cell:Target Cell Conjugates for Immunofluorescence and Flow Cytometric Assays. For IF, 3×10^5 target cells and 3×10^5 CD8 OT-I effector T cells were mixed and centrifuged at 500 rpm for 5 min at 4 °C in serum-free medium in the presence of vehicle, LPA, cytochalasin D, latrunculin A, colchicine, or nocodazole, followed by incubation at 37 °C for the indicated time prior to plating on poly-L-lysine–coated (Sigma) coverslips. Cells were fixed with 4% paraformaldehyde in PBS, permeabilized with 0.15% Triton Surfact-Amps, Fc receptor blocked, stained with the indicated primary antibodies and appropriate secondary antibodies, and cured with Prolong Diamond anti-fade with DAPI. Cells were imaged using an Eclipse TE2000-E (Nikon) with a 100× oil-immersion objective, captured with SlideBook6 software (3i, Intelligent Imaging Innovations, Inc.), and analyzed with ImageJ/FIJI (ImageJ open source software, https://imagej.net).

For flow cytometric analysis of T cell:conjugate cell formation and analysis of acetylated and detyrosinated tubulin, effector CD8 T cells and target cells were differentially dye labeled with carboxyfluorscein succinimidyl ester (CFSE) and eFluor670, respectively, prior to mixing 1×10^6 target cells with 1×10^6 CD8 OT-I effector T cells and centrifugation at 500 rpm for 5 min at 4 °C in serum-free medium in the presence of vehicle, LPA, nocodazole, or Trichostatin A (TSA). Cells were incubated at 37 °C for the indicated time, briefly vortexed to disrupt nonspecific conjugates, fixed with 4% paraformaldehyde, permeabilized with PBS/0.1% saponin/0.5% BSA for 10 min, and stained with anti–acetyl-α-tubulin or anti-detyrosinated tubulin followed by an anti-rabbit secondary. Flow cytometric analysis utilized a BD Fortessa with BD FACSDiva software for data collection and FlowJo software for analysis.

Statistical Analysis. Results are displayed as means ± SEM. *P* value was considered significant if $P \leq 0.05$ and was determined via paired or unpaired Student's *t* test as indicated in each figure legend. Three or more independent experiments were executed for each dataset as indicated in the figure legends. Imaging data consisted of multiple cells being analyzed from three or more independent experiments. Analysis was performed using GraphPad Prism version 9.0 and/or Excel.

Additional methods, antibodies, reagents, and analysis of immunofluorescent data can be found in *SI Appendix*.

Data Availability. All study data are included in the article and/or *SI Appendix*.

ACKNOWLEDGMENTS. We thank the healthy donors who provided samples for this research. This work was supported by NIH Grants AI143261 (R.M.T.), AI124474 (R.P.), AI152535 (R.P.), and AI125553 (J.J.) and a grant from the Cancer League of Colorado (R.M.T.).

Author affiliations: [a]Department of Immunology and Microbiology, University of Colorado School of Medicine, Aurora, CO 80045; [b]Department of Drug Discovery Medicine, Kyoto University Graduate School of Medicine, Kyoto 606-8507, Japan; [c]Barbara Davis Center for Diabetes, University of Colorado, Aurora, CO 80045; and [d]Department of Immunology and Genomic Medicine, National Jewish Health, Denver, CO 80206

1. A. C. Anderson, N. Joller, V. K. Kuchroo, Lag-3, Tim-3, and TIGIT: Co-inhibitory receptors with specialized functions in immune regulation. *Immunity* **44**, 989–1004 (2016).
2. J. Attanasio, E. J. Wherry, Costimulatory and coinhibitory receptor pathways in infectious disease. *Immunity* **44**, 1052–1068 (2016).
3. S. P. Kubli, T. Berger, D. V. Araujo, L. L. Siu, T. W. Mak, Beyond immune checkpoint blockade: Emerging immunological strategies. *Nat. Rev. Drug Discov.* **20**, 899–919 (2021).
4. M. Gotoh *et al.*, Controlling cancer through the autotaxin-lysophosphatidic acid receptor axis. *Biochem. Soc. Trans.* **40**, 31–36 (2012).
5. D. Mathew, R. M. Torres, Lysophosphatidic acid is an inflammatory lipid exploited by cancers for immune evasion via mechanisms similar and distinct from CTLA-4 and PD-1. *Front. Immunol.* **11**, 531910 (2021).
6. G. B. Mills, W. H. Moolenaar, The emerging role of lysophosphatidic acid in cancer. *Nat. Rev. Cancer* **3**, 582–591 (2003).
7. K. R. Baumforth *et al.*, Induction of autotaxin by the Epstein-Barr virus promotes the growth and survival of Hodgkin lymphoma cells. *Blood* **106**, 2138–2146 (2005).
8. N. Watanabe *et al.*, Both plasma lysophosphatidic acid and serum autotaxin levels are increased in chronic hepatitis C. *J. Clin. Gastroenterol.* **41**, 616–623 (2007).
9. G. Gaud, R. Lesourne, P. E. Love, Regulatory mechanisms in T cell receptor signalling. *Nat. Rev. Immunol.* **18**, 485–497 (2018).
10. A. H. Courtney, W. L. Lo, A. Weiss, T. C. R. Signaling, TCR signaling: Mechanisms of initiation and propagation. *Trends Biochem. Sci.* **43**, 108–123 (2018).
11. N. deSouza, J. Cui, M. Dura, T. V. McDonald, A. R. Marks, A function for tyrosine phosphorylation of type 1 inositol 1,4,5-trisphosphate receptor in lymphocyte activation. *J. Cell Biol.* **179**, 923–934 (2007).
12. J. Liang *et al.*, Tespa1 regulates T cell receptor-induced calcium signals by recruiting inositol 1,4,5-trisphosphate receptors. *Nat. Commun.* **8**, 15732 (2017).
13. H. Takayama, M. V. Sitkovsky, Antigen receptor-regulated exocytosis in cytotoxic T lymphocytes. *J. Exp. Med.* **166**, 725–743 (1987).
14. A. T. Pores-Fernando, A. Zweifach, Calcium influx and signaling in cytotoxic T-lymphocyte lytic granule exocytosis. *Immunol. Rev.* **231**, 160–173 (2009).
15. A. Babich, J. K. Burkhardt, Coordinate control of cytoskeletal remodeling and calcium mobilization during T-cell activation. *Immunol. Rev.* **256**, 80–94 (2013).
16. S. Kumari, S. Curado, V. Mayya, M. L. Dustin, T cell antigen receptor activation and actin cytoskeleton remodeling. *Biochim. Biophys. Acta* **1838**, 546–556 (2014).
17. D. Thumkeo *et al.*, mDia1/3-dependent actin polymerization spatiotemporally controls LAT phosphorylation by Zap70 at the immune synapse. *Sci. Adv.* **6**, eaay2432 (2020).
18. L. Andrés-Delgado *et al.*, INF2 promotes the formation of detyrosinated microtubules necessary for centrosome reorientation in T cells. *J. Cell Biol.* **198**, 1025–1037 (2012).
19. K. M. Eisenmann *et al.*, T cell responses in mammalian diaphanous-related formin mDia1 knockout mice. *J. Biol. Chem.* **282**, 25152–25158 (2007).
20. D. Sakata *et al.*, Impaired T lymphocyte trafficking in mice deficient in an actin-nucleating protein, mDia1. *J. Exp. Med.* **204**, 2031–2038 (2007).
21. L. Andrés-Delgado, O. M. Antón, M. A. Alonso, Centrosome polarization in T cells: A task for formins. *Front. Immunol.* **4**, 191 (2013).
22. F. Bartolini, G. G. Gundersen, Formins and microtubules. *Biochim. Biophys. Acta* **1803**, 164–173 (2010).
23. V. Calvo, M. Izquierdo, Role of actin cytoskeleton reorganization in polarized secretory traffic at the immunological synapse. *Front. Cell Dev. Biol.* **9**, 629097 (2021).

24. T. Kuwabara, Y. Matsui, F. Ishikawa, M. Kondo, Regulation of T-cell signaling by post-translational modifications in autoimmune disease. *Int. J. Mol. Sci.* **19**, 819 (2018).
25. S. Knowlden, S. N. Georas, The autotaxin-LPA axis emerges as a novel regulator of lymphocyte homing and inflammation. *J. Immunol.* **192**, 851–857 (2014).
26. K. Schmitz *et al.*, Dysregulation of lysophosphatidic acids in multiple sclerosis and autoimmune encephalomyelitis. *Acta Neuropathol. Commun.* **5**, 42 (2017).
27. C. Li *et al.*, Targeting the RhoA-ROCK pathway to regulate T-cell homeostasis in hypoxia-induced pulmonary arterial hypertension. *Pulm. Pharmacol. Ther.* **50**, 111–122 (2018).
28. S. Lin *et al.*, Autotaxin determines colitis severity in mice and is secreted by B cells in the colon. *FASEB J.* **33**, 3623–3635 (2019).
29. M. Kondo *et al.*, Lysophosphatidic acid regulates the differentiation of Th2 cells and its antagonist suppresses allergic airway inflammation. *Int. Arch. Allergy Immunol.* **182**, 1–13 (2021).
30. F. Bartolini *et al.*, The formin mDia2 stabilizes microtubules independently of its actin nucleation activity. *J. Cell Biol.* **181**, 523–536 (2008).
31. F. Leve *et al.*, Lysophosphatidic acid induces a migratory phenotype through a crosstalk between RhoA-Rock and Src-FAK signalling in colon cancer cells. *Eur. J. Pharmacol.* **671**, 7–17 (2011).
32. J. van Unen *et al.*, Plasma membrane restricted RhoGEF activity is sufficient for RhoA-mediated actin polymerization. *Sci. Rep.* **5**, 14693 (2015).
33. J. Rubenfeld *et al.*, Lysophosphatidic acid enhances interleukin-13 gene expression and promoter activity in T cells. *Am. J. Physiol. Lung Cell. Mol. Physiol.* **290**, L66–L74 (2006).
34. H. Kanda *et al.*, Autotaxin, an ectoenzyme that produces lysophosphatidic acid, promotes the entry of lymphocytes into secondary lymphoid organs. *Nat. Immunol.* **9**, 415–423 (2008).
35. S. K. Oda *et al.*, Lysophosphatidic acid inhibits CD8 T cell activation and control of tumor progression. *Cancer Immunol. Res.* **1**, 245–255 (2013).
36. S. A. Knowlden *et al.*, Regulation of T cell motility in vitro and in vivo by LPA and LPA2. *PLoS One* **9**, e101655 (2014).
37. T. Katakai, T. Kinashi, Microenvironmental control of high-speed interstitial T cell migration in the lymph node. *Front. Immunol.* **7**, 194 (2016).
38. D. Mathew *et al.*, LPA_5 is an inhibitory receptor that suppresses CD8 T-cell cytotoxic function via disruption of early TCR signaling. *Front. Immunol.* **10**, 1159 (2019).
39. M. L. Dustin, Stop and go traffic to tune T cell responses. *Immunity* **21**, 305–314 (2004).
40. W. A. Dar, S. J. Knechtle, CXCR3-mediated T-cell chemotaxis involves ZAP-70 and is regulated by signalling through the T-cell receptor. *Immunology* **120**, 467–485 (2007).
41. K. Schaeuble, M. A. Hauser, E. Singer, M. Groettrup, D. F. Legler, Cross-talk between TCR and CCR7 signaling sets a temporal threshold for enhanced T lymphocyte migration. *J. Immunol.* **187**, 5645–5652 (2011).
42. J. F. Camargo *et al.*, CCR5 expression levels influence NFAT translocation, IL-2 production, and subsequent signaling events during T lymphocyte activation. *J. Immunol.* **182**, 171–182 (2009).
43. K. N. Kremer, A. Kumar, K. E. Hedin, G alpha i2 and ZAP-70 mediate RasGRP1 membrane localization and activation of SDF-1-induced T cell functions. *J. Immunol.* **187**, 3177–3185 (2011).
44. K. N. Kremer *et al.*, TCR-CXCR4 signaling stabilizes cytokine mRNA transcripts via a PREX1-Rac1 pathway: Implications for CTCL. *Blood* **130**, 982–994 (2017).
45. J. Hu *et al.*, Lysophosphatidic acid receptor 5 inhibits B cell antigen receptor signaling and antibody response. *J. Immunol.* **193**, 85–95 (2014).
46. G. Tigyi, Aiming drug discovery at lysophosphatidic acid targets. *Br. J. Pharmacol.* **161**, 241–270 (2010).
47. Y. Xu *et al.*, Lysophosphatidic acid as a potential biomarker for ovarian and other gynecologic cancers. *JAMA* **280**, 719–723 (1998).
48. Y. Klymenko *et al.*, Lysophosphatidic acid modulates ovarian cancer multicellular aggregate assembly and metastatic dissemination. *Sci. Rep.* **10**, 10877 (2020).
49. S. Reinartz *et al.*, Cell type-selective pathways and clinical associations of lysophosphatidic acid biosynthesis and signaling in the ovarian cancer microenvironment. *Mol. Oncol.* **13**, 185–201 (2019).
50. A. M. Westermann *et al.*, Malignant effusions contain lysophosphatidic acid (LPA)-like activity. *Ann. Oncol.* **9**, 437–442 (1998).
51. Y. J. Xiao *et al.*, Electrospray ionization mass spectrometry analysis of lysophospholipids in human ascitic fluids: Comparison of the lysophospholipid contents in malignant vs nonmalignant ascitic fluids. *Anal. Biochem.* **290**, 302–313 (2001).
52. K. A. Hogquist *et al.*, T cell receptor antagonist peptides induce positive selection. *Cell* **76**, 17–27 (1994).
53. J. W. Copeland, R. Treisman, The diaphanous-related formin mDia1 controls serum response factor activity through its effects on actin polymerization. *Mol. Biol. Cell* **13**, 4088–4099 (2002).
54. T. Katakai, N. Kondo, Y. Ueda, T. Kinashi, Autotaxin produced by stromal cells promotes LFA-1-independent and Rho-dependent interstitial T cell motility in the lymph node paracortex. *J. Immunol.* **193**, 617–626 (2014).
55. N. B. Thillaiappan, A. P. Chavda, S. C. Tovey, D. L. Prole, C. W. Taylor, Ca^{2+} signals initiate at immobile IP_3 receptors adjacent to ER-plasma membrane junctions. *Nat. Commun.* **8**, 1505 (2017).
56. M. Geyer *et al.*, Microtubule-associated protein EB3 regulates IP3 receptor clustering and Ca(2+) signaling in endothelial cells. *Cell Rep.* **12**, 79–89 (2015).
57. J. C. Stinchcombe, E. Majorovits, G. Bossi, S. Fuller, G. M. Griffiths, Centrosome polarization delivers secretory granules to the immunological synapse. *Nature* **443**, 462–465 (2006).
58. J. Yi *et al.*, Centrosome repositioning in T cells is biphasic and driven by microtubule end-on capture-shrinkage. *J. Cell Biol.* **202**, 779–792 (2013).
59. C. Janke, M. M. Magiera, The tubulin code and its role in controlling microtubule properties and functions. *Nat. Rev. Mol. Cell Biol.* **21**, 307–326 (2020).
60. A. Hashimoto-Tane *et al.*, Dynein-driven transport of T cell receptor microclusters regulates immune synapse formation and T cell activation. *Immunity* **34**, 919–931 (2011).
61. J. M. Serrador *et al.*, HDAC6 deacetylase activity links the tubulin cytoskeleton with immune synapse organization. *Immunity* **20**, 417–428 (2004).
62. A. Palazzo, B. Ackerman, G. G. Gundersen, Cell biology: Tubulin acetylation and cell motility. *Nature* **421**, 230 (2003).
63. T. Nagasaki, G. G. Gundersen, Depletion of lysophosphatidic acid triggers a loss of oriented detyrosinated microtubules in motile fibroblasts. *J. Cell Sci.* **109**, 2461–2469 (1996).
64. A. F. Palazzo, T. A. Cook, A. S. Alberts, G. G. Gundersen, mDia mediates Rho-regulated formation and orientation of stable microtubules. *Nat. Cell Biol.* **3**, 723–729 (2001).
65. S. B. Thompson *et al.*, Formin-like 1 mediates effector T cell trafficking to inflammatory sites to enable T cell-mediated autoimmunity. *eLife* **9**, e58046 (2020).
66. M. Huse, E. J. Quann, M. M. Davis, Shouts, whispers and the kiss of death: Directional secretion in T cells. *Nat. Immunol.* **9**, 1105–1111 (2008).
67. M. Huse, B. F. Lillemeier, M. S. Kuhns, D. S. Chen, M. M. Davis, T cells use two directionally distinct pathways for cytokine secretion. *Nat. Immunol.* **7**, 247–255 (2006).
68. L. H. M. Geraldo *et al.*, Role of lysophosphatidic acid and its receptors in health and disease: Novel therapeutic strategies. *Signal Transduct. Target. Ther.* **6**, 45 (2021).
69. T. S. Gomez *et al.*, Formins regulate the actin-related protein 2/3 complex-independent polarization of the centrosome to the immunological synapse. *Immunity* **26**, 177–190 (2007).
70. K. L. Singleton *et al.*, Spatiotemporal patterning during T cell activation is highly diverse. *Sci. Signal.* **2**, ra15 (2009).
71. S. J. Heasman, L. M. Carlin, S. Cox, T. Ng, A. J. Ridley, Coordinated RhoA signaling at the leading edge and uropod is required for T cell transendothelial migration. *J. Cell Biol.* **190**, 553–563 (2010).
72. A. T. Ritter *et al.*, Actin depletion initiates events leading to granule secretion at the immunological synapse. *Immunity* **42**, 864–876 (2015).
73. E. V. Tibaldi, R. Salgia, E. L. Reinherz, CD2 molecules redistribute to the uropod during T cell scanning: Implications for cellular activation and immune surveillance. *Proc. Natl. Acad. Sci. U.S.A.* **99**, 7582–7587 (2002).
74. F. Bartolini *et al.*, An mDia1-INF2 formin activation cascade facilitated by IQGAP1 regulates stable microtubules in migrating cells. *Mol. Biol. Cell* **27**, 1797–1808 (2016).
75. J. A. Gorman *et al.*, The cytoskeletal adaptor protein IQGAP1 regulates TCR-mediated signaling and filamentous actin dynamics. *J. Immunol.* **188**, 6135–6144 (2012).
76. W. M. Lim, Y. Ito, K. Sakata-Sogawa, M. Tokunaga, CLIP-170 is essential for MTOC repositioning during T cell activation by regulating dynein localisation on the cell surface. *Sci. Rep.* **8**, 17447 (2018).
77. Y. Wen *et al.*, EB1 and APC bind to mDia to stabilize microtubules downstream of Rho and promote cell migration. *Nat. Cell Biol.* **6**, 820–830 (2004).
78. C. Guntermann, D. R. Alexander, CTLA-4 suppresses proximal TCR signaling in resting human CD4(+) T cells by inhibiting ZAP-70 Tyr(319) phosphorylation: A potential role for tyrosine phosphatases. *J. Immunol.* **168**, 4420–4429 (2002).
79. K. A. Sheppard *et al.*, PD-1 inhibits T-cell receptor induced phosphorylation of the ZAP70/CD3zeta signalosome and downstream signaling to PKCtheta. *FEBS Lett.* **574**, 37–41 (2004).
80. N. Acharya, C. Sabatos-Peyton, A. C. Anderson, Tim-3 finds its place in the cancer immunotherapy landscape. *J. Immunother. Cancer* **8**, e000911 (2020).
81. D. D. Billadeau, J. C. Nolz, T. S. Gomez, Regulation of T-cell activation by the cytoskeleton. *Nat. Rev. Immunol.* **7**, 131–143 (2007).
82. M. M. Morgan *et al.*, Superantigen-induced T cell:B cell conjugation is mediated by LFA-1 and requires signaling through Lck, but not ZAP-70. *J. Immunol.* **167**, 5708–5718 (2001).
83. J. C. Nolz *et al.*, WAVE2 regulates high-affinity integrin binding by recruiting vinculin and talin to the immunological synapse. *Mol. Cell. Biol.* **27**, 5986–6000 (2007).
84. A. Tsun *et al.*, Centrosome docking at the immunological synapse is controlled by Lck signaling. *J. Cell Biol.* **192**, 663–674 (2011).
85. N. B. Martín-Cófreces *et al.*, Role of Fyn in the rearrangement of tubulin cytoskeleton induced through TCR. *J. Immunol.* **176**, 4201–4207 (2006).
86. S. J. Lord, K. B. Velle, R. D. Mullins, L. K. Fritz-Laylin, SuperPlots: Communicating reproducibility and variability in cell biology. *J. Cell Biol.* **219**, e202001064 (2020).